# Measurement of jet production in deep inelastic scattering and NNLO determination of the strong coupling at ZEUS[†]

## $\alpha_s$ workshop 2024

**Florian Lorkowski on behalf of the ZEUS collaboration**
`florian.lorkowski@physik.uzh.ch`

Deutsches Elektronen-Synchrotron DESY[‡]

ZEUS

**February 6, 2024**

---

[†] EPJC 83, 1082 (2023). arXiv:`2309.02889`
[‡] Now at University of Zürich

# Motivation

## Deep inelastic scattering

### Deep inelastic scattering

- Inclusive deep inelastic scattering (DIS) measurements in lepton-hadron collisions ($ep \to eX$) are essential to determine the parton distribution functions (PDFs) of the proton ($xf$). At leading order:

$$\frac{\mathrm{d}^2\sigma^{\pm}_{\text{NC DIS}}}{\mathrm{d}x_{\mathrm{Bj}}\mathrm{d}Q^2} = \frac{2\pi\alpha^2}{x_{\mathrm{Bj}}Q^4}\left(\underbrace{Y_+F_2(x_{\mathrm{Bj}},Q^2)}_{\sim xq+x\bar{q}} \mp \underbrace{Y_-x_{\mathrm{Bj}}F_3(x_{\mathrm{Bj}},Q^2)}_{\sim xq-x\bar{q}} - \underbrace{y^2F_{\mathrm{L}}(x_{\mathrm{Bj}},Q^2)}_{\sim xg\times\alpha_s}\right)$$

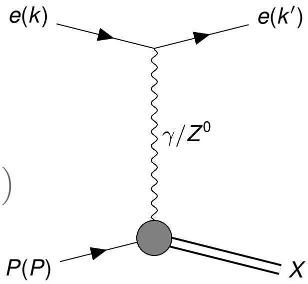

⇒ By measuring $F_2$ and $F_3$, the quark- and antiquark-distributions, $xq$ and $x\bar{q}$, can be probed

- By measuring $F_{\mathrm{L}}$ or using scaling violations in DGLAP equations the product of the gluon distribution $xg$ and the strong coupling constant $\alpha_s$ can be determined
- Using higher-order terms, the two can be disentangled to some extent, but a strong correlation remains

# Motivation

## Inclusive jet production

### Jet measurements

- Already at leading order,[†] jet production in DIS is sensitive to the strong coupling independently of the gluon distribution (upper graph)
- Additionally, jet production can also be used to further constrain the gluon distribution (lower graph)
- Inclusive jet measurements are especially well suited for precision determinations of the strong coupling constant due to their small uncertainties on both the experimental and theoretical side

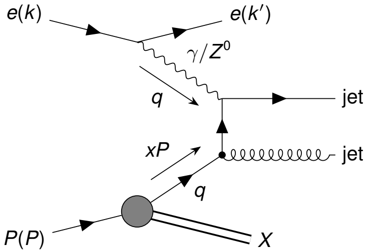

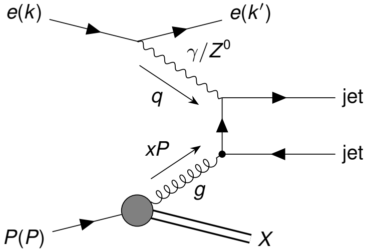

---

[†] Leading order in the Breit frame; see slide 5

# Theory of deep inelastic scattering

## Definitions

### Deep inelastic scattering

- Scattering of leptons off hadrons at high momentum transfer $Q^2$

$$e(k) + P(P) \rightarrow e(k') + p'(p') + X$$

- Boson acts as point-like probe of the hadron

$p'$ . . . Scattered hadronic system

$X$ . . . Proton remnant

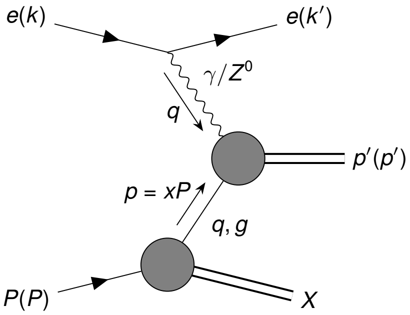

### Kinematic quantities

| | |
|---|---|
| $Q^2 = -q^2 = -(k' - k)^2$ | Boson virtuality/ Momentum transfer |
| $x_{\mathrm{Bj}} = \dfrac{Q^2}{2P \cdot q}$ | Bjorken scaling parameter |
| $y = \dfrac{P \cdot q}{P \cdot k}$ | Inelasticity |

# Theory of deep inelastic scattering

## Parton distribution functions

- To predict cross sections of lepton-hadron collisions, one needs
  - The boson-parton cross sections $\hat{\sigma}$ (calculable using perturbative QCD)
  - The parton content of the hadron (unknown but assumed to be universal for each hadron); parameterised using PDFs $xf$
- PDFs can only be determined from fits to measurements
- Adding jet data to the fit allows a simultaneous determination of $\alpha_s$ and the PDFs

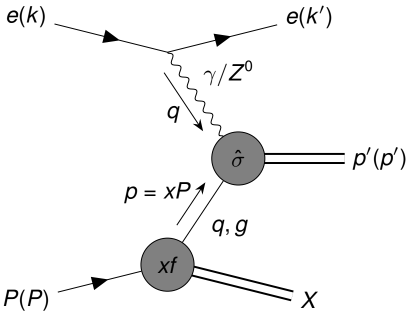

# Theory of deep inelastic scattering

## Breit frame

- Single jets may arise purely from QED, which is uninteresting for studies of QCD
- To suppress these events: require minimum transverse momentum in Breit frame

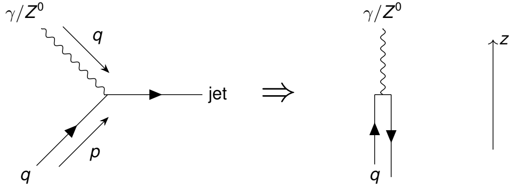

In the **Breit frame**, the parton and boson collide head-on

$$q^\mu = \begin{pmatrix} 0 \\ 0 \\ 0 \\ -Q \end{pmatrix}$$

$$p^\mu = \begin{pmatrix} Q/2 \\ 0 \\ 0 \\ Q/2 \end{pmatrix}$$

# Theory of deep inelastic scattering
## Breit frame

- Single jets may arise purely from QED, which is uninteresting for studies of QCD
- To suppress these events: require minimum transverse momentum in Breit frame

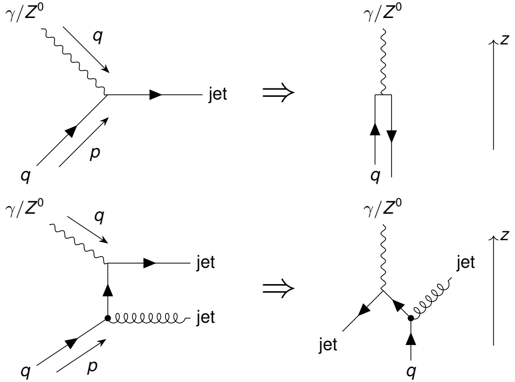

In the **Breit frame**, the parton and boson collide head-on

$$q^\mu = \begin{pmatrix} 0 \\ 0 \\ 0 \\ -Q \end{pmatrix}$$

$$p^\mu = \begin{pmatrix} Q/2 \\ 0 \\ 0 \\ Q/2 \end{pmatrix}$$

- Lowest order process: produce two jets of equal transverse momentum (“dijet”)
- Inclusive jets: count each jet individually; events can contribute multiple times

# Experiment
## HERA and ZEUS

### HERA accelerator

- World's only lepton-hadron collider so far
- Located at DESY in Hamburg, Germany
- Two run periods:
  - HERA I: 1992 – 2000
  - HERA II: 2003 – 2007
- Circular collider of length 6336 m
- Collide electrons/positrons at 27.5 GeV with protons at 920 GeV $\rightarrow \sqrt{s} = 318$ GeV

### ZEUS detector

- General purpose particle detector
- Integrated luminosity during HERA II: 347 $\text{pb}^{-1}$
- High-resolution uranium-scintillator calorimeter allows precise measurement of jet energies

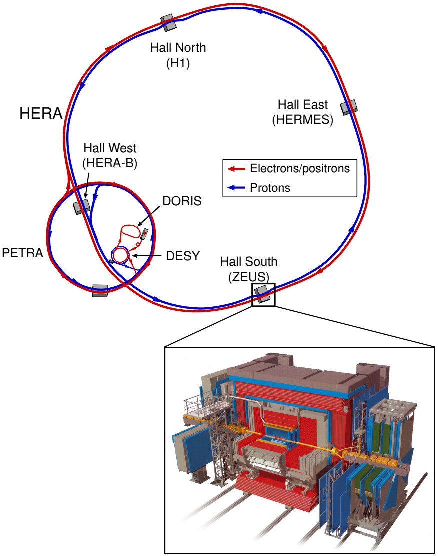

# Measurement

## Cross section definition

- Inclusive jets, clustered using $k_\perp$ algorithm and $p_\perp$-weighted scheme in Breit frame
- Use entire HERA II dataset (347 $\mathrm{pb}^{-1}$)
- Analysis phase space

$$
\begin{aligned}
150\,\mathrm{GeV}^2 < \quad & Q^2 \quad < 15\,000\,\mathrm{GeV}^2 \\
0.2 < \quad & y \quad < 0.7
\end{aligned}
$$

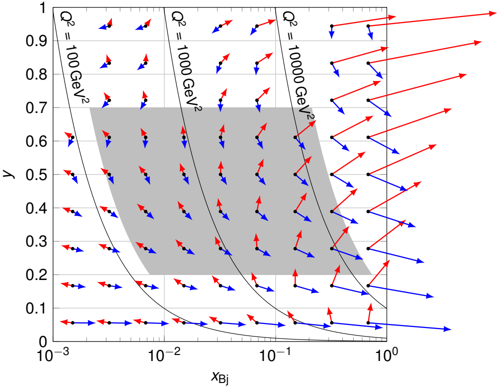

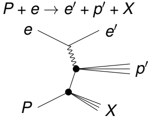

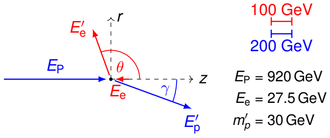

# Measurement
## Cross section definition

- Inclusive jets, clustered using $k_\perp$ algorithm and $p_\perp$-weighted scheme in Breit frame
- Use entire HERA II dataset ($347\,\mathrm{pb}^{-1}$)
- Analysis phase space

$$
\begin{aligned}
150\,\mathrm{GeV}^2 < {} & Q^2 < 15\,000\,\mathrm{GeV}^2 \\
0.2 < {} & y < 0.7 \\
7\,\mathrm{GeV} < {} & p_{\perp,\mathrm{Breit}} < 50\,\mathrm{GeV} \\
-1 < {} & \eta_\mathrm{lab} < 2.5
\end{aligned}
$$

- Hadron-level jets
- Weak-boson exchange included
- QED Born-level (higher-order radiative effects removed)

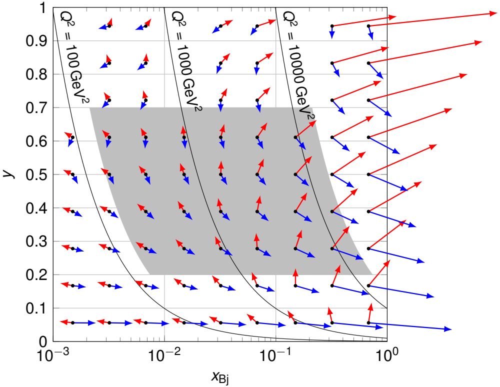

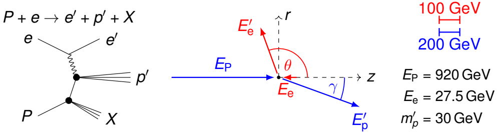

$E_P = 920\,\mathrm{GeV}$
$E_e = 27.5\,\mathrm{GeV}$
$m'_p = 30\,\mathrm{GeV}$

# Measurement

## Simulation

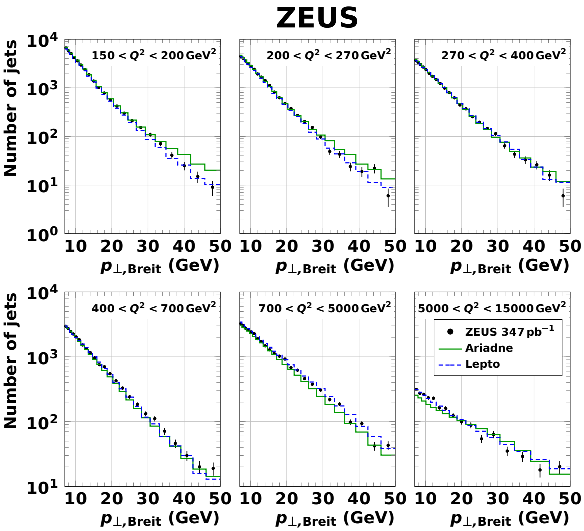

- Reconstructed jets corrected to hadron level via two-dimensional matrix unfolding procedure using response matrices obtained from Monte Carlo samples
  - ARIADNE: colour-dipole model
  - LEPTO: leading-log parton cascade
- After reweighting, the models give a good description of the data across the entire phase space
- Performed cross-check using bin-by-bin correction; results are very consistent

# Measurement

## Systematic uncertainties

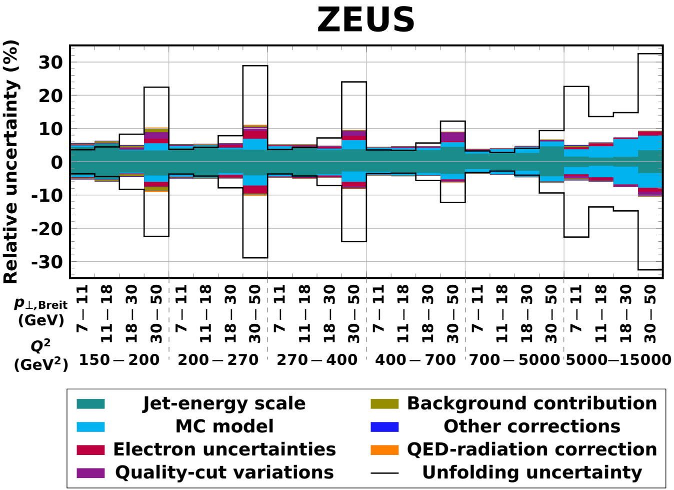

- Systematic uncertainty mostly dominated by jet-energy scale (uncertainty of MC detector simulation)
- In high-$p_{\perp,\mathrm{Breit}}$ or high-$Q^2$ region, other uncertainties become relevant/dominant
- Unfolding uncertainty appears large in low-statistics region
- Bins with large unfolding uncertainty usually strongly anti-correlated

# Measurement

## Systematic uncertainties

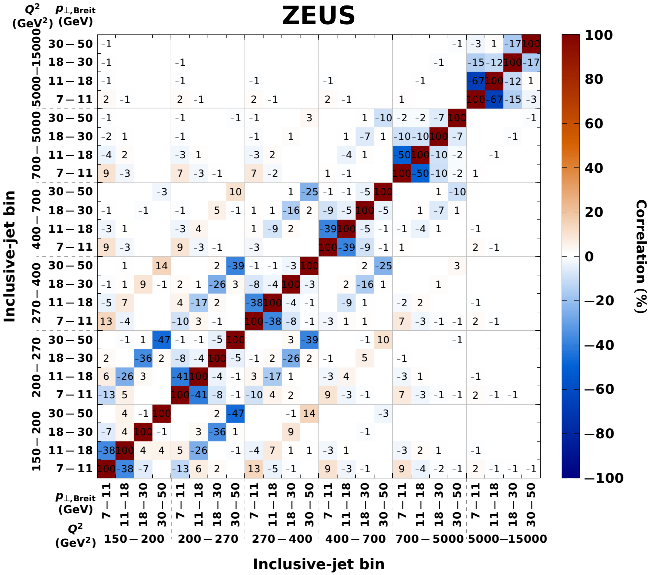

| $Q^2$ (GeV$^2$) | $p_{\perp,\mathrm{Breit}}$ (GeV) | 150 – 200 | | | | 200 – 270 | | | | 270 – 400 | | | | 400 – 700 | | | | 700 – 5000 | | | | 5000–15000 | | | |
|---|---|---|---|---|---|---|---|---|---|---|---|---|---|---|---|---|---|---|---|---|---|---|---|---|---|
| | | 7 – 11 | 11 – 18 | 18 – 30 | 30 – 50 | 7 – 11 | 11 – 18 | 18 – 30 | 30 – 50 | 7 – 11 | 11 – 18 | 18 – 30 | 30 – 50 | 7 – 11 | 11 – 18 | 18 – 30 | 30 – 50 | 7 – 11 | 11 – 18 | 18 – 30 | 30 – 50 | 7 – 11 | 11 – 18 | 18 – 30 | 30 – 50 |
| 5000–15000 | 30 – 50 | -1 | | | | | | | | | | | | | | | | | | | -1 | -3 | 1 | -17 | 100 |
| | 18 – 30 | -1 | | | | -1 | | | | | | | | | | | | | | -1 | | -15 | -12 | 100 | -17 |
| | 11 – 18 | -1 | | | | -1 | | | | -1 | | | | -1 | | | | | -1 | | | -67 | 100 | -12 | 1 |
| | 7 – 11 | 2 | -1 | | | 2 | -1 | | | 2 | -1 | | | 2 | -1 | | | 1 | | | | 100 | -67 | -15 | -3 |
| 700 – 5000 | 30 – 50 | -1 | | | | -1 | | | -1 | -1 | | | 3 | | | 1 | -10 | -2 | -2 | -7 | 100 | | | | -1 |
| | 18 – 30 | -2 | 1 | | | -1 | | | | -1 | | 1 | | | 1 | -7 | 1 | -10 | -10 | 100 | -7 | | | -1 | |
| | 11 – 18 | -4 | 2 | | | -3 | 1 | | | -3 | 2 | | | | -4 | 1 | | -50 | 100 | -10 | -2 | | -1 | | |
| | 7 – 11 | 9 | -3 | | | 7 | -3 | -1 | | 7 | -2 | | | 1 | -1 | | | 100 | -50 | -10 | -2 | 1 | | | |
| 400 – 700 | 30 – 50 | | | | -3 | | | | 10 | | | 1 | -25 | -1 | -1 | -5 | 100 | | | 1 | -10 | | | | |
| | 18 – 30 | -1 | | -1 | | -1 | | 5 | -1 | 1 | 1 | -16 | 2 | -9 | -5 | 100 | -5 | | 1 | -7 | 1 | | | | |
| | 11 – 18 | -3 | 1 | | | -3 | 4 | | | 1 | -9 | 2 | | -39 | 100 | -5 | -1 | -1 | -4 | 1 | | -1 | | | |
| | 7 – 11 | 9 | -3 | | | 9 | -3 | -1 | | -3 | | | | 100 | -39 | -9 | -1 | 1 | | | | 2 | -1 | | |
| 270 – 400 | 30 – 50 | | 1 | | 14 | | | 2 | -39 | -1 | -1 | -3 | 100 | | | 2 | -25 | | | | 3 | | | | |
| | 18 – 30 | -1 | 1 | 9 | -1 | 2 | 1 | -26 | 3 | -8 | -4 | 100 | -3 | | 2 | -16 | 1 | | | 1 | | | | | |
| | 11 – 18 | -5 | 7 | | | 4 | -17 | 2 | | -38 | 100 | -4 | -1 | | -9 | 1 | | -2 | 2 | | | -1 | | | |
| | 7 – 11 | 13 | -4 | | | -10 | 3 | -1 | | 100 | -38 | -8 | -1 | -3 | 1 | 1 | | 7 | -3 | -1 | -1 | 2 | -1 | | |
| 200 – 270 | 30 – 50 | | -1 | 1 | -47 | -1 | -1 | -5 | 100 | | | 3 | -39 | | | -1 | 10 | | | | -1 | | | | |
| | 18 – 30 | 2 | | -36 | 2 | -8 | -4 | 100 | -5 | -1 | 2 | -26 | 2 | -1 | | 5 | | -1 | | | | | | | |
| | 11 – 18 | 6 | -26 | 3 | | -41 | 100 | -4 | -1 | 3 | -17 | 1 | | -3 | 4 | | | -3 | 1 | | | -1 | | | |
| | 7 – 11 | -13 | 5 | | | 100 | -41 | -8 | -1 | -10 | 4 | 2 | | 9 | -3 | -1 | | 7 | -3 | -1 | -1 | 2 | -1 | -1 | |
| 150 – 200 | 30 – 50 | | 4 | -1 | 100 | | | 2 | -47 | | | -1 | 14 | | | | -3 | | | | | | | | |
| | 18 – 30 | -7 | 4 | 100 | -1 | | 3 | -36 | 1 | | | 9 | | | | -1 | | | | | | | | | |
| | 11 – 18 | -38 | 100 | 4 | 4 | 5 | -26 | | -1 | -4 | 7 | 1 | 1 | -3 | 1 | | | -3 | 2 | 1 | | -1 | | | |
| | 7 – 11 | 100 | -38 | -7 | | -13 | 6 | 2 | | 13 | -5 | -1 | | 9 | -3 | -1 | | 9 | -4 | -2 | -1 | 2 | -1 | -1 | -1 |

- Systematic uncertainty mostly dominated by jet-energy scale (uncertainty of MC detector simulation)
- In high-$p_{\perp,\mathrm{Breit}}$ or high-$Q^2$ region, other uncertainties become relevant/dominant
- Unfolding uncertainty appears large in low-statistics region
- Bins with large unfolding uncertainty usually strongly anti-correlated

# Measurement

## Theoretical predictions

### Theoretical predictions

- Cross section predictions are calculated at NNLO
- Matrix elements calculated using NNLOJET[†]
- PDFs taken from HERAPDF2.0Jets NNLO[‡]
- $\alpha_s(M_Z^2) = 0.1155$, $\mu_r^2 = \mu_f^2 = Q^2 + p_\perp^2$
- Predictions corrected for hadronisation and $Z^0$-exchange

### Theoretical uncertainties

- Six point scale variation by factor 2
- PDF uncertainty (fit, model, parameterisation)
- Statistical uncertainty of matrix element generation
- Hadronisation correction uncertainty

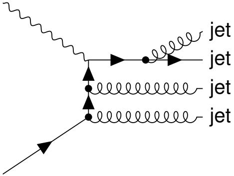

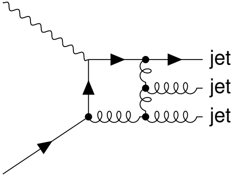

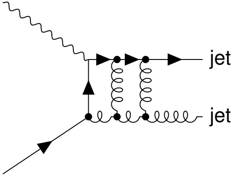

---

[†] JHEP 2017, 18 (2017). arXiv:`1703.05977`

[‡] EPJC 82, 243 (2022). arXiv:`2112.01120`

# Cross sections

## Measured inclusive jet cross sections

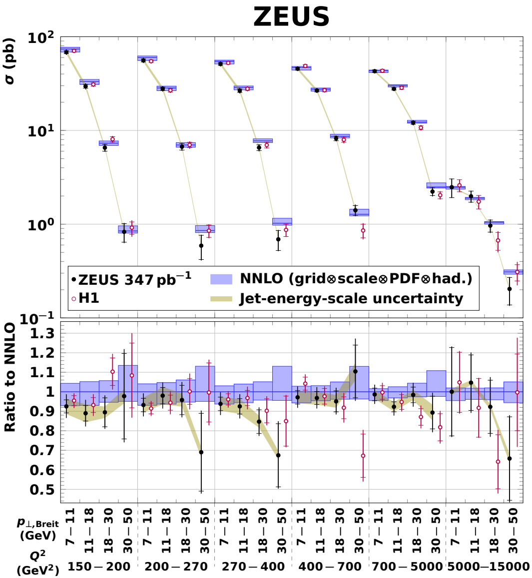

- Measured cross sections are compatible with previous measurement from H1 collaboration[‡] and uncertainties are comparable
- Measurements are compatible with NNLO QCD predictions and show similar trends relative to the theory
- Inner error bars: unfolding uncertainty; outer error bars: total uncertainty

---

[‡] EPJC 75, 65 (2015). arXiv:`1406.4709`

# Cross sections

## QED radiation

### Treatment of QED radiation

- Predictions for jet production available at QED Born-level (running coupling included, but no radiative corrections)
- In the data, have initial- and final-state QED radiation, especially on the electron line
- Standard procedure: apply ‘correction’ to the data, to convert it to QED Born-level
- Usually, this cannot be undone, such that data can only ever be compared to QED Born-level predictions
- This analysis: apply correction in a reversible way and provide additional, alternative correction that facilitates more comprehensive comparisons

→ Data can be compared to NNLO QCD+NLO EW predictions, when they become available in the future[†]

**QED Born-level**

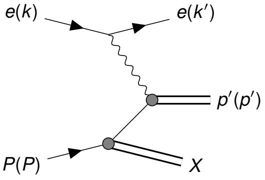

**QED radiation**

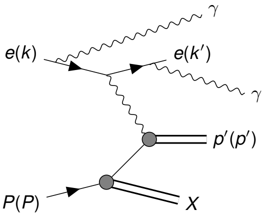

---

[†] DIS at NLO EW already available: CPC 94, 2 p.128 (1996). arXiv:`hep-ph/9511434`

# QCD analysis
## Strategy

- Simultaneous fit of PDF parameters and $\alpha_s(M_Z^2)$ at NNLO
- Datasets used
  - H1+ZEUS combined inclusive DIS[†]
  - ZEUS HERA I inclusive jets at high $Q^{2\,‡}$
  - ZEUS HERA I+II dijets at high $Q^{2\,§}$
  - **ZEUS HERA II inclusive jets at high $Q^2$**
- Inclusion of additional jet data is expected to reduce uncertainty of $\alpha_s(M_Z^2)$
- Statistical correlations between ZEUS HERA II jet datasets taken into account via correlation matrix
- Use HERAPDF parameterisation of PDFs ($f = g, u_v, d_v, \bar{U}, \bar{D}$)

$$xf(x) = A_f x^{B_f}(1-x)^{C_f}(1 + D_f x + E_f x^2)$$

- Use settings similar to HERAPDF2.0Jets NNLO (central scales, cuts, model parameters, treatment of hadronisation and theory grid uncertainty)

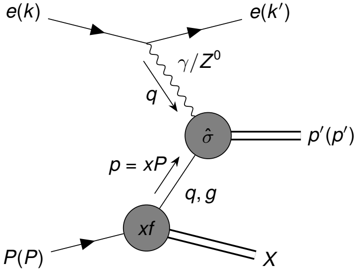

---

[†] EPJC 75, 580 (2015) arXiv::`1506.06042`

[‡] PLB 547, 164 (2002) arXiv::`hep-ex/0208037`

[§] EPJC 70, 965 (2010) arXiv::`1010.6167`

# QCD analysis

## Parton distribution functions

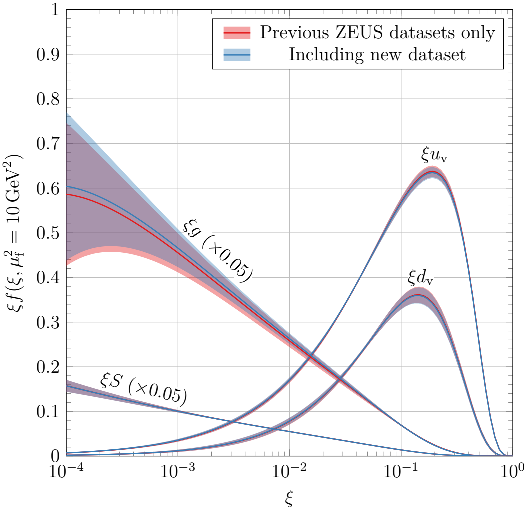

- Perform two fits and compare PDFs:
  1. HERA inclusive DIS dataset + previous ZEUS jet datasets
  2. Also include newly measured ZEUS HERA II inclusive jet datasets
- Shown is experimental/fit uncertainty
- Gluon distribution is slightly constrained
- As expected, quark distributions are not significantly affected/constrained
- Uncertainty of gluon distribution appears much larger than in HERAPDF,[†] because $\alpha_\mathrm{s}(M_Z^2)$ is left free in the fit

---

[†] E.g. fig. 4 of arXiv:`2112.01120`

# QCD analysis
## Strong coupling

For reference, HERAPDF2.0Jets NNLO found

$$\alpha_s(M_Z^2) = \mathbf{0.1156} \pm 0.0011 \text{ (exp/fit) } {}^{+0.0001}_{-0.0002} \text{ (model/parameterisation) } \pm 0.0029 \text{ (scale)}$$

This analysis

$$\boxed{\alpha_s(M_Z^2) = \mathbf{0.1143} \pm 0.0014 \text{ (exp/fit) } {}^{+0.0004}_{-0.0008} \text{ (model/parameterisation) } {}^{+0.0012}_{-0.0005} \text{ (scale)}}$$

- Central value is compatible with HERAPDF and with PDG world average
- Increased experimental uncertainty, due to fewer jet datasets used
- Significantly decreased scale uncertainty, due to absence of low-$Q^2$ jet data
    - Cross-section scale-dependence assumed as fully correlated between all jet measurements
    - When fitting points far away from each other in phase space, the cross-section scale-dependence can be much less correlated or even anti-correlated

# QCD analysis
## Strong coupling

For reference, HERAPDF2.0Jets NNLO found

$$\alpha_s(M_Z^2) = 0.1156 \pm \mathbf{0.0011}\ \textbf{(exp/fit)}\ {}^{+0.0001}_{-0.0002}\ \text{(model/parameterisation)} \pm 0.0029\ \text{(scale)}$$

This analysis

$$\boxed{\alpha_s(M_Z^2) = 0.1143 \pm \mathbf{0.0014}\ \textbf{(exp/fit)}\ {}^{+0.0004}_{-0.0008}\ \text{(model/parameterisation)}\ {}^{+0.0012}_{-0.0005}\ \text{(scale)}}$$

- Central value is compatible with HERAPDF and with PDG world average
- Increased experimental uncertainty, due to fewer jet datasets used
- Significantly decreased scale uncertainty, due to absence of low-$Q^2$ jet data
    - Cross-section scale-dependence assumed as fully correlated between all jet measurements
    - When fitting points far away from each other in phase space, the cross-section scale-dependence can be much less correlated or even anti-correlated

# QCD analysis
## Strong coupling

For reference, HERAPDF2.0Jets NNLO found

$$\alpha_s(M_Z^2) = 0.1156 \pm 0.0011\ \text{(exp/fit)}\ {}^{+0.0001}_{-0.0002}\ \text{(model/parameterisation)} \pm \mathbf{0.0029}\ \textbf{(scale)}$$

This analysis

$$\boxed{\alpha_s(M_Z^2) = 0.1143 \pm 0.0014\ \text{(exp/fit)}\ {}^{+0.0004}_{-0.0008}\ \text{(model/parameterisation)}\ {}^{+\mathbf{0.0012}}_{-\mathbf{0.0005}}\ \textbf{(scale)}}$$

- Central value is compatible with HERAPDF and with PDG world average
- Increased experimental uncertainty, due to fewer jet datasets used
- Significantly decreased scale uncertainty, due to absence of low-$Q^2$ jet data
  - Cross-section scale-dependence assumed as fully correlated between all jet measurements
  - When fitting points far away from each other in phase space, the cross-section scale-dependence can be much less correlated or even anti-correlated

# QCD analysis
## Alternative treatment of scale uncertainty

- Alternative treatment: assume scale dependence is half correlated between all measurements
- Despite absence of low-$Q^2$ jet data in the fit, additional reduction is significant

$$\alpha_s(M_Z^2) = 0.1143 \pm \ldots {}^{+0.0012}_{-0.0005}\,\text{(scale)}$$
$$\downarrow$$
$$\alpha_s(M_Z^2) = 0.1142 \pm \ldots {}^{+0.0006}_{-0.0004}\,\text{(scale)}$$

# QCD analysis

## Alternative treatment of scale uncertainty

- Alternative treatment: assume scale dependence is half correlated between all measurements
- Despite absence of low-$Q^2$ jet data in the fit, additional reduction is significant

$$\alpha_s(M_Z^2) = 0.1143 \pm \ldots {}^{+0.0012}_{-0.0005} \text{ (scale)}$$

$$\downarrow$$

$$\alpha_s(M_Z^2) = 0.1142 \pm \ldots {}^{+0.0006}_{-0.0004} \text{ (scale)}$$

- Reduced scale uncertainty leads to one of the most precise collider measurements of $\alpha_s(M_Z^2)$[†]

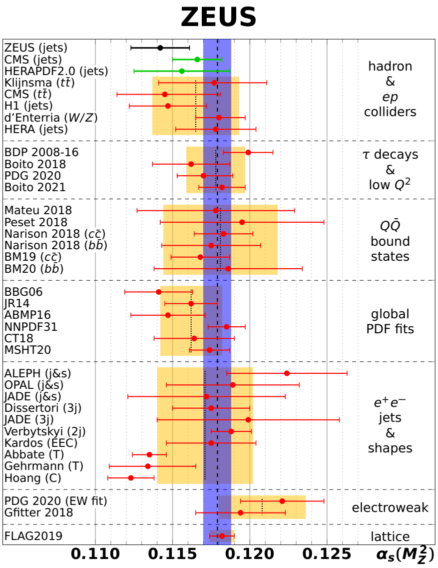

---

[†] PTEP 2022, 8, 083C01 (2022)

# QCD analysis
## Comparison to HERAPDF

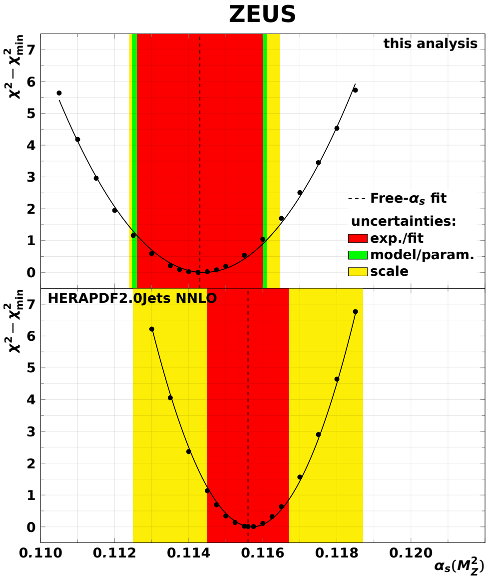

- Upper panel: $\chi^2(\alpha_s(M_Z^2))$-scan, alongside result from $\alpha_s(M_Z^2)$-free fit
  $\rightarrow$ excellent agreement
- Lower panel: analogous figure from HERAPDF2.0Jet NNLO
- Need better treatment of scale uncertainty, so that we can combine small scale uncertainty from ZEUS with small experimental uncertainty from HERAPDF

# QCD analysis

## Running of the strong coupling

- Strong coupling depends on the scale at which it is evaluated. At leading order

$$\alpha_\mathrm{s}(\mu^2) = \frac{\alpha_\mathrm{s}(\mu_0^2)}{1 + \alpha_\mathrm{s}(\mu_0^2) b_0 \log\left(\frac{\mu^2}{\mu_0^2}\right)}$$

- ‘Measure’ this curve to test if QCD is the correct theory to describe strong interaction
  - Assign each jet point a scale
  - Form subsets of jet points with similar scales
  - For each subset, perform a single-parameter $\alpha_\mathrm{s}$ fit using fixed PDFs

# QCD analysis

## Running of the strong coupling

- Strong coupling depends on the scale at which it is evaluated. At leading order

$$\alpha_{\mathrm{s}}(\mu^2) = \frac{\alpha_{\mathrm{s}}(\mu_0^2)}{1 + \alpha_{\mathrm{s}}(\mu_0^2) b_0 \log\left(\frac{\mu^2}{\mu_0^2}\right)}$$

- ‘Measure’ this curve to test if QCD is the correct theory to describe strong interaction
  - Assign each jet point a scale
  - Form subsets of jet points with similar scales
  - For each subset, perform a single-parameter $\alpha_{\mathrm{s}}$ fit using fixed PDFs
- Observe no deviation from QCD prediction

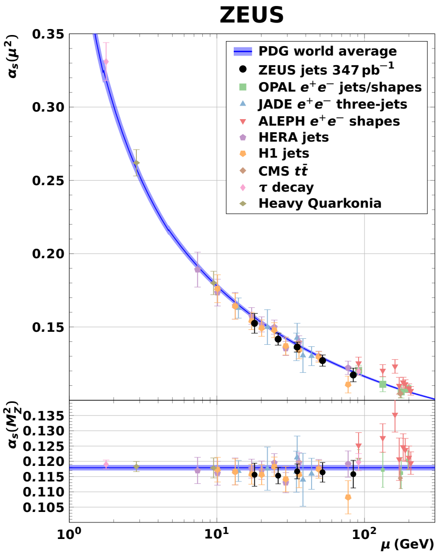

# Summary

## Cross section measurement

### Cross section measurement

- Performed precision measurement of inclusive jet cross sections in deep inelastic scattering at ZEUS
- Used more than 70% of the entire available luminosity at ZEUS
- Cross sections are compatible with the corresponding H1 measurement and NNLO QCD theory
- New dataset is an ideal ingredient for precision determinations of $\alpha_s(M_Z^2)$ in QCD fits

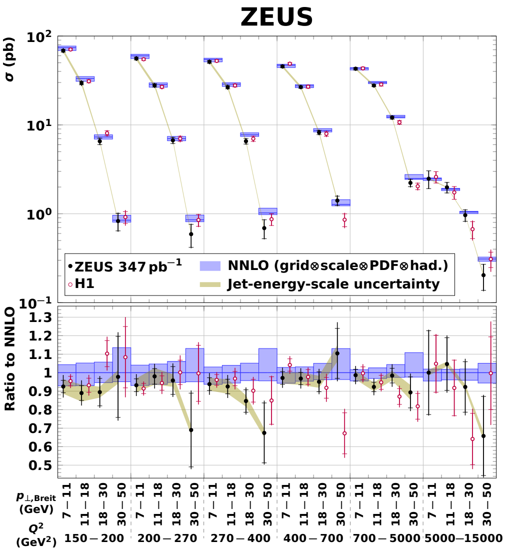

# Summary
## NNLO QCD analysis

### QCD analysis

- Dataset used in $\alpha_s(M_Z^2)$ determination at NNLO
- Achieved very precise measurement of $\alpha_s(M_Z^2)$

$$\alpha_s(M_Z^2) = 0.1142 \pm 0.0019$$

  due to
  - Newly measured inclusive jet dataset
  - Restriction to high-$Q^2$ jet data in the fit
  - Improved treatment of theoretical uncertainty
- Investigated scale-dependence of strong coupling and found results consistent with NNLO QCD prediction

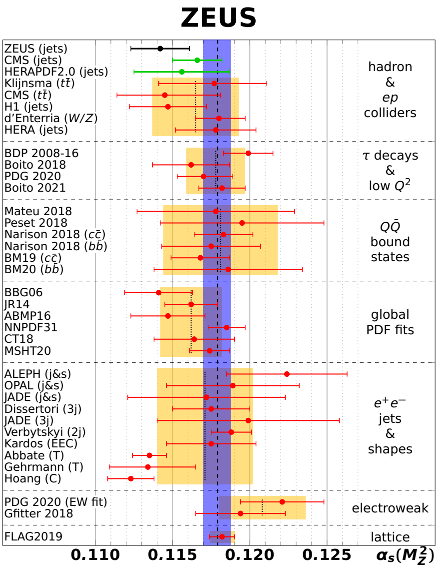

# Summary

## NNLO QCD analysis

### QCD analysis

- Dataset used in $\alpha_s(M_Z^2)$ determination at NNLO
- Achieved very precise measurement of $\alpha_s(M_Z^2)$

  $$\alpha_s(M_Z^2) = 0.1142 \pm 0.0019$$

  due to

  - Newly measured inclusive jet dataset
  - Restriction to high-$Q^2$ jet data in the fit
  - Improved treatment of theoretical uncertainty
- Investigated scale-dependence of strong coupling and found results consistent with NNLO QCD prediction

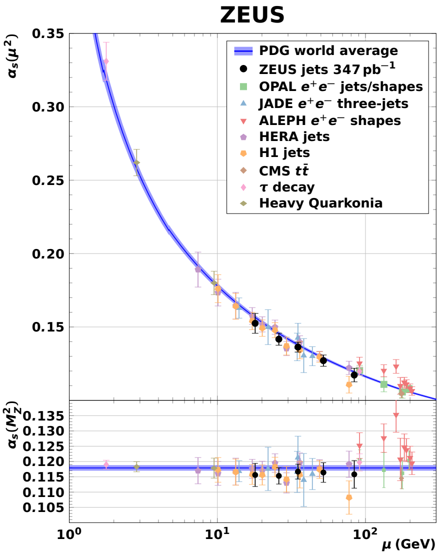

# QCD analysis
## Fit settings

### Fit settings

|  | **NLO** | **NNLO** |
|---|---|---|
|  | Model parameters |  |
| $f_s$ | $0.4 \pm 0.1$ |  |
| $m_c$ [GeV] | $1.46\,^{+0.04}_{-\text{symmetrise}}$ | $1.41\,^{+0.04}_{-\text{symmetrise}}$ |
| $m_b$ [GeV] | $4.3 \pm 0.10$ | $4.2 \pm 0.10$ |
| $Q^2_{\text{min}}$ [GeV$^2$] | $3.5\,^{+1.5}_{-1.0}$ |  |
|  | Parameterisation |  |
| $\mu^2_{\text{f0}}$ [GeV$^2$] | $1.9\,^{-0.3}_{+\text{symmetrise}}$ |  |
| Additional parameters | all missing $D$ and $E$ parameters <br> $(D_g, E_g, D_{u_v}, D_{d_v}, E_{d_v}, E_{\bar{U}}, D_{\bar{D}}, E_{\bar{D}})$ |  |
|  | Scales |  |
| $\mu_\text{f}^2$ | $Q^2$ | $Q^2 + p_\perp^2$ |
| $\mu_\text{r}^2$ | $(Q^2 + p_\perp^2)/2$ |  |

### Parameterisation

$$xg(x) = A_g x^{B_g}(1-x)^{C_g} - A'_g x^{B'_g}(1-x)^{C'_g}$$

$$xu_v(x) = A_{u_v} x^{B_{u_v}}(1-x)^{C_{u_v}}(1 + E_{u_v} x^2)$$

$$xd_v(x) = A_{d_v} x^{B_{d_v}}(1-x)^{C_{d_v}}$$

$$x\bar{U}(x) = A_{\bar{U}} x^{B_{\bar{U}}}(1-x)^{C_{\bar{U}}}(1 + D_{\bar{U}} x)$$

$$x\bar{D}(x) = A_{\bar{D}} x^{B_{\bar{D}}}(1-x)^{C_{\bar{D}}}$$

### Constraints

$A_g$ determined by sum rules

$A_{u_v}$ determined by sum rules

$A_{d_v}$ determined by sum rules

$C'_g = 25$

$B_{\bar{U}} = B_{\bar{D}}$

$A_{\bar{U}} = A_{\bar{D}}(1 - f_s)$

# QCD analysis

## Goodness of fit

| **Dataset** | **Partial $\chi^2$ / Number of points** |
|---|---|
| HERA NC $e^+p$ DIS, $E_P = 920\,\text{GeV}$ | 447.65 / 377 |
| HERA NC $e^+p$ DIS, $E_P = 820\,\text{GeV}$ | 64.99 / 70 |
| HERA NC $e^+p$ DIS, $E_P = 575\,\text{GeV}$ | 219.16 / 254 |
| HERA NC $e^+p$ DIS, $E_P = 460\,\text{GeV}$ | 216.58 / 204 |
| HERA NC $e^-p$ DIS, $E_P = 920\,\text{GeV}$ | 219.88 / 159 |
| HERA CC $e^+p$ DIS, $E_P = 920\,\text{GeV}$ | 47.52 / 39 |
| HERA CC $e^-p$ DIS, $E_P = 920\,\text{GeV}$ | 51.73 / 42 |
| HERA I inclusive jets | 26.38 / 30 |
| HERA I/II dijets | 14.65 / 16 |
| HERA II inclusive jets | 14.98 / 24 |

| | |
|---|---|
| Shifts of correlated systematics | 96.24 |
| Global $\chi^2$ per degree of freedom | 1418.93 / 1200 = 1.182 |

| | |
|---|---|
| HERAPDF2.0 NNLO | 1363 / 1131 = 1.205 |
| HERAPDF2.0Jets NNLO | 1614 / 1348 = 1.197 |